Thermal analysis to assess pozzolanic activity of calcined kaolinitic clays

Alejandra Tironi, Monica A. Trezza, Alberto N. Scian & Edgardo F. Irassar

Journal of Thermal Analysis and Calorimetry
An International Forum for Thermal Studies

ISSN 1388-6150

J Therm Anal Calorim
DOI 10.1007/s10973-014-3816-1

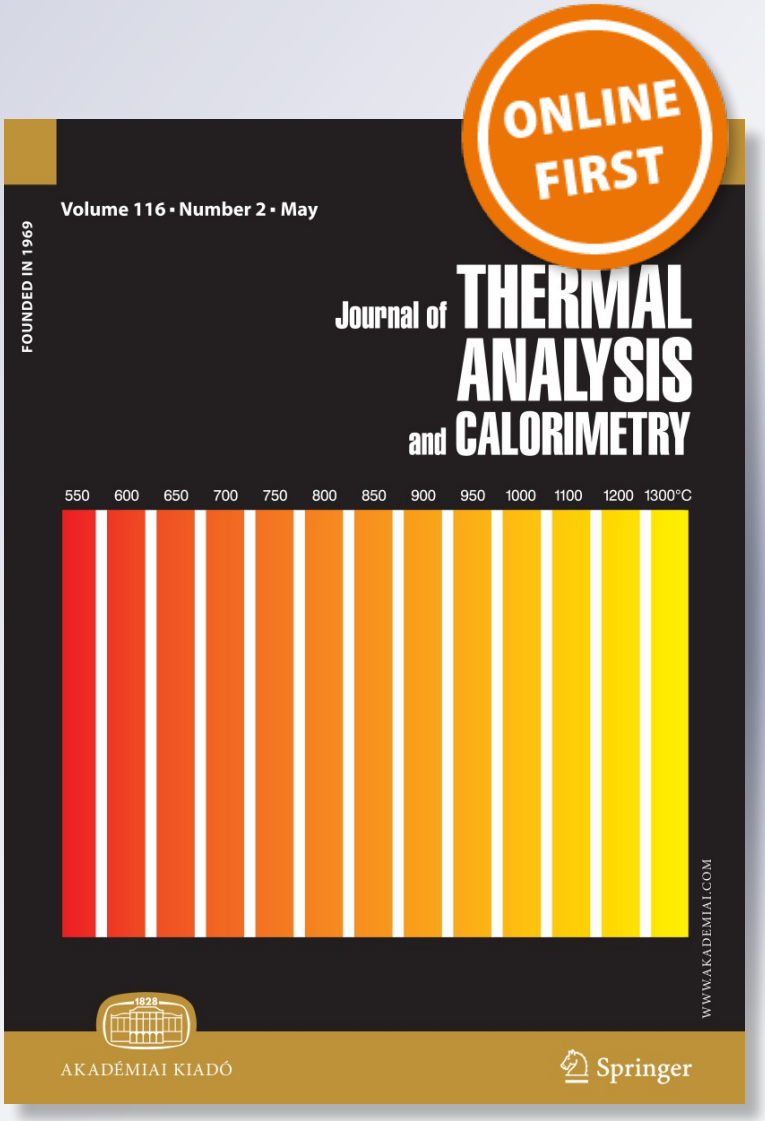

Springer

J Therm Anal Calorim
DOI 10.1007/s10973-014-3816-1

Thermal analysis to assess pozzolanic activity of calcined kaolinitic clays

Alejandra Tironi · Monica A. Trezza · Alberto N. Scian · Edgardo F. Irassar

Received: 18 September 2013 / Accepted: 4 April 2014

Abstract The use of calcined clays as partial replacement of cement is encouraged since it promotes the reduction of the green-house gas emission and the energy requirement of cement-based material, maintaining or enhancing the mechanical properties and the durable performance of these materials. In this paper, the use of thermal methods—DTA/TG and calorimetry—to select and to evaluate two kaolinitic clays for their use as pozzolanic materials was explored. The content and crystallinity of kaolinite in clays can be determined by DTA/TG analysis, and this technique is also suitable to select the calcination temperature for complete kaolinite dehydroxylation. Calorimetric analysis on blended cements (30 % by mass of replacement) can differentiate the reactivity of calcined kaolinitic clays. Results show that more reactive calcined kaolinitic clay develops the second and third peaks earlier than those of PC with great intensity and high acceleration. The reactivity of calcined clays is associated to raw materials containing kaolinite with high structural disorder that determines calcined clays with large specific surface area, high grindability, and small mean particles size (d_{50}) for the same grinding objective. Finally, the DTA/TG analysis can determine the type and the amount of hydrated phases obtained at different ages to evaluate the pozzolanic reaction of calcined clay in accordance with the standardized pozzolanic activity index.

A. Tironi · M. A. Trezza · E. F. Irassar (✉)
Facultad de Ingeniería, Universidad Nacional del Centro de la Provincia de Buenos Aires, B7400 JWI Olavarría, Argentina
e-mail: firassar@fio.unicen.edu.ar

A. N. Scian
Centro de Tecnología de Recursos Minerales y Cerámica, CONICET La Plata - UNLP, Gonnet, Argentina

Keywords Kaolinite · Calcined clay · Pozzolanic activity · Cement · DTA/TG · Isothermal calorimetry

Introduction

Portland cement (PC) is a basic component of concrete and mortar widely used in the construction of buildings and infrastructure systems. In addition, PC production causes serious environmental problems, such as the CO_2 emissions and the energy consumption during its process [1, 2].

The use of calcined clays as partial replacement of cement is encouraged since it promotes the reduction of the green-house gas emission and the energy requirement for cement-based material, maintaining or enhancing their mechanical properties and the durable performance of these materials. Among the different clays, when they are thermally activated, kaolinitic clays appear as highly reactive pozzolan after appropriate grinding. The thermal treatment (550–900 °C) produces the dehydroxylation of kaolinite in the clay obtaining an amorphous aluminosilicate phase (AS_2), called metakaolinite (MK) that presents a good pozzolanic activity [3–5].

When kaolinitic-calcined clays are incorporated to Portland cement, several effects (physical and chemical) are observed on the hydration process at ambient temperature. The main physical effects are (a) the dilution effect, which is equivalent to an increase in the water-to-cement ratio, inversely proportional to the replacement level; and (b) the filler effect, which is related to fine grains interposed between cement grains separating and dispersing the reactive cement grains; they also act as nucleation centers for the CH, accelerating the

Published online: 27 April 2014

dissolution process and stimulating the hydration of cement. The main chemical effect is the pozzolanic reaction between the MK and the CH, producing a cementing compound like C–S–H and some alumina-hydrated phases that depend on the CH available. According to Murat [6], the reaction produces calcium aluminate hydrate when the CH content is higher, Eq. (1), and strätlingite, when the CH content is lower, Eq. (2).

$$AS_2 + 6CH + 9H \rightarrow 2C-S-H + C_4AH_{13} \quad (1)$$

$$AS_2 + 3CH + 6H \rightarrow C-S-H + C_2ASH_8 \quad (2)$$

Depending on the replacement level, the content of MK in calcined clays, the reactivity of MK, its specific surface area, and the acceleration promoted on cement hydration, the pozzolanic reaction can compensate the adverse effect of dilution during early age [7, 8].

The objective of this study is to use the DTA/TG and calorimetry techniques to select and to evaluate kaolinitic clays for their use as pozzolanic materials, determining the kaolinite content and structural features, the calcination conditions, and the differences in the pozzolanic activities with Portland cement.

Experimental

Materials

Two natural kaolinitic clays from Argentina were examined: K1 collected from primary deposits (La Rioja, Province); and K2 collected from a sedimentary deposit (Río Negro Province) [9, 10]. The chemical composition, determined by ICP-AES analysis in an external laboratory (ALS, Argentina), and the loss on ignition of clays are reported in Table 1. A Portland cement (PC) classified as CEM I according to EN-197 [11] was used to prepare blended pastes and mortars. Its chemical composition determined by the X-ray fluorescence is reported in Table 1. The mineralogical composition of clinker calculated using the Bogue's formula was $C_3S = 47$ %, $C_2S = 22$ %, $C_3A = 8$ %, and $C_4AF = 9$ %. The minor component in CEM I was the limestone addition (less than 5 %), and the Blaine specific surface area of Portland cement was 383 $m^2\ kg^{-1}$.

Methods

Raw clays

The argillaceous minerals present in kaolinitic natural clays were identified by differential thermal analysis (DTA) and corroborated by X-ray diffraction (XRD). The kaolinite content was determined by the thermogravimetric method (TG) [12]. DTA-TG analysis was carried out using a NETZCH STA 409 thermobalance, and XRD analysis was performed on Philips PW 3710 diffractometer operating with Cu $K\alpha$ radiation at 40 kV and 20 mA.

The crystallinity of kaolinite in the clays was evaluated using different indexes obtained from DTA and XRD patterns. The slope ratio index (SR) is calculated as the ratio between the slope of the descending branch of the kaolinite dexhydroxylation peak in the DTA curve (350–700 °C) and the slope of the ascending branch of the same peak. The SR characterizes the presence of surface defects: For SR = 1, the peak is symmetric, and the kaolinite does not present many surface defects, and when the SR is greater than 2, the mineral presents many surface defects [13]. The calculated indexes based on XRD were full width half maximum (FWHM-001 and FWHM-002) [14, 15], Hinckley (HI) [16] and random defects (R2) [17].

Calcined clays

Calcination was carried out in a programmable laboratory furnace Indef 272 using a fixed bed technique. The calcination temperature was selected from the DTA analysis as discussed later.

Calcined clays were ground in a mortar-type mill (Fritsch Pulverisette 2) until fineness was 80 % lower than 45 μm. In this material, the particle size distribution was determined using Malvern Mastersizer 2000 laser particle size analyzer, and the d_{90}, d_{50}, and d_{10} diameters were calculated. Complementary, the specific surface area (SS) was determined using BET technique (Micromeritics ASAP 2020) and the Blaine method [18]. The K1 and K2-clays calcined and ground are named as MK1 and MK2, respectively.

Hydration of blended cement

The hydration of pastes containing blended cement was studied at early and later ages. The pastes were prepared

Table 1 Chemical composition of kaolinitic clays and Portland cement (PC), in percent

Materials	SiO_2	Al_2O_3	Fe_2O_3	CaO	MgO	SO_3	Na_2O	K_2O	TiO_2	LOI
K1 (ICP)	45.9	37.0	0.77	0.08	0.12	–	0.06	0.40	0.99	13.30
K2 (ICP)	51.4	31.3	0.92	0.40	0.19	–	0.36	0.38	1.42	12.15
PC (XRF)	19.9	5.5	3.00	58.62	3.81	3.22	0.70	1.11	0.34	3.19

using a water-to-cementitious material ratio (w/cm) of 0.5 and cured in sealed plastic bags at 20 °C. The blended cements were formulated replacing PC by 30 % by mass of ground kaolinitic-calcined clays (30MK1 and 30MK2). A neat Portland cement paste was prepared as reference. This replacement level was selected according to the pozzolanic activity test for calcined clays (thermal-activated pozzolan). In this test, the blending cement tested has a replacement level of pozzolan by cement ranging from 25 to 35 % in mass or volume depending on the standard used. This paper is derived from previous investigation on the pozzolanic properties of calcined clay with different argillaceous minerals [7], where the kaolinite content was from 16 to 94 %, and the national standard specifies blended cement with 30 % in weight of pozzolan.

The hydration studies at early age were performed during 48 h using an isothermal conduction calorimetry operating at 20 °C. Thereafter, the progress of hydration compounds was studied by thermal analysis (DTA/TG) on fragment of paste sample at 2, 7, and 28 days. To identify the hydrated phases at the characteristic times of the calorimetric curve and later ages, XRD analysis on powdered samples of paste was performed using a Philips PW 3710 diffractometer. At the stipulated time, fragments of paste were immersed in acetone to stop the hydration. Thereafter, they were placed overnight in an oven at 40 °C and then cooled in a desiccator. Finally, the sample was ground to pass a 45-μm sieve and the XRD-holder was backfilled to prevent the crystal preferred orientation.

Compressive strength

Compressive strength of blended cements was determined on mortars cubes (25 × 25 × 25 mm^3) made with standard sand (1:3) and w/cm of 0.50. The strength activity index (SAI) was calculated as the ratio of the compressive strength of the blended cement to the strength of the Portland cement at the same age [7].

Results and discussion

Raw clays

The DTA curve of pure kaolinite shows an endothermic peak in the temperature range of 500–700 °C due to the mineral dehydroxylation [15], and it is associated with a mass loss of 13.76 % [12]. The results obtained by DTA/TG for the kaolinitic clays are presented in Fig. 1, and the kaolinite content determined by TG is reported in Table 2. K1-clay has the highest kaolinite content (99 %), and both clays can be classified as kaolin since kaolinite content is higher than 75 % [19]. XRD patterns of both clays confirmed that the main argillaceous mineral is kaolinite, and the impurities are quartz and anatase for K1-clay; and quartz, anatase, and illite for K2-clay.

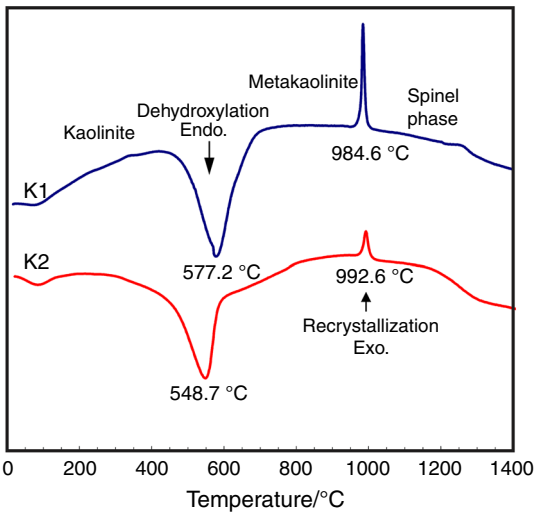

Fig. 1 DTA curves of kaolinitic clays

Table 2 Kaolinite content in clays determined by DTA/TG and crystallinity indices of kaolinite obtaining by DTA and XRD

Technique		K1	K2	
DTA/TG	Kaolinite/ %	99	87	
	Índex			Range analysis
DTA	SR	1.76	3.20	≈1.0 O; ≥2.0 D
XRD	FWHM-001	0.21	0.58	< 0.3 O; >0.4 D
	FWHM-002	0.20	0.64	< 0.3 O; >0.4 D
	HI	1.19	0.36	> 1.5 O; <0.5 D
	R2	1.16	0.77	0.7 D to 1.2 O

O order structure, *D* disorder structure

The values of SR, FWHM-001, FWHM-002, HI, and R2 indexes are summarized in Table 2. The five indexes classify K2-clay and K1-clay as containing disordered and ordered structures, respectively. The SR index determined by DTA has been sufficient to determine the degree of structural order/disorder in kaolinite.

Summarizing, the content and crystallinity of kaolinite in the clay can be determined by DTA/TG analysis. Both variables have large influence on the pozzolanic activity of calcined clays. Then, the compressive strengths at different ages depend on the amorphous material derived from kaolinite content in clay, the structural order/disorder of kaolinite, and the specific surface area, all of which determine the rate of pozzolanic reaction. The specific surface area of calcined clay has a large influence on the hydration at very early age; the structural disorder of

Table 3 Physical characteristics of Portland cement (PC) and kaolinitic-calcined clays

Materials	d_{90}/μm	d_{50}/μm	d_{10}/μm	SS Blaine/ $m^2\ kg^{-1}$	SS BET/ $m^2\ kg^{-1}$
PC	49.7	15.4	2.3	383	–
MK1	131.4	19.6	1.3	997	8,117
MK2	47.0	7.4	2.1	1,365	38,997

kaolinite is more important at 28 days; and the kaolinite content has greater mass at later ages [7].

Calcined kaolinitic clays

The selected calcination temperatures for K1 and K2 clays were 700 and 750 °C, respectively. The maximum temperature for the complete dehydroxylation of kaolinite and its transformation into an amorphous phase metakaolinite occurs at 700 °C for K1 (Fig. 1). For this clay, the exothermic peak at 985 °C is assigned to the metakaolinite recrystallization in the spinel phase. When the temperature is higher than 700 °C, the reduction of the amorphous phase is detected by Fourier-transformed infrared spectroscopy (FTIR), attributed to the structural rearrangement to form the crystalline phase [20]. For K2, the temperature was 750 °C, and both results were corroborated by pozzolanic activity test [21]. Using the emanation thermal analysis (ETA), Balek and Murat [22] determined the temperature for the maximum structural disorder of metakaolinite. It was ~700 °C for clay with well-crystallized kaolinite (called ANG), and ~750 °C for clay with poor-crystallized kaolinite (called FON). They concluded that the disorder of MK decreases when the temperature increases up to 850 °C, and it can be correlated with the "recrystallization"/"sintering" of the pseudo-lattice of metakaolinite leading to an extensive segregation of alumina and silica. In previous study [21], employing different techniques, the authors confirm that the optimal temperature for the high pozzolanic activity was higher for kaolinite with disordered structure.

MK1 obtained from K1-clay with high content of ordered kaolinite has a high content of metakaolinite, but it has a low specific surface area (BET and Blaine), and it is too hard to grind, causing a large maximum particle size for the same grinding objective (20 % on 45-μm sieve). Then, the mean particle size (d_{50}) of MK1 (19.6 μm) is greater than the d_{50} of MK2 (7.4 μm), and their coarser particles (d_{90}) are too larger (see Table 3). This coarse particle size distribution can affect negatively the pozzolanic activity of MK1-calcined clays. On the other hand, MK2 obtained from K2-clay with low content of disordered kaolinite has a larger specific surface area than that of MK1 (4.8 times larger for SS BET and 1.4 times larger for SS Blaine) and finer particle size distribution for the same grinding procedure (Table 3).

The degree of structural disorder in the kaolinite determined by SR-index from DTA analysis is an indication of the primary or the secondary origin of geological deposit. The order/disorder of the kaolinite structure determines the specific surface area, the grindability, and the mean particle size of the calcined clays.

Hydration at early age

Figure 2 shows the calorimetric curves for pastes containing PC, 30MK1, and 30MK2. For the heat release rate versus time curve (Fig. 2a), the overall progress of hydration can be divided into five periods: (1) dissolution and wetting, (2) dormant, (3) acceleration, (4) aluminate reaction, and (5) de-acceleration.

The first period is characterized by a high exothermic signal that occurs immediately after mixing the water with the cement. It is attributed to the wetting, the dissolution of C_3S, and the formation of initial ettringite (Ett) on the surface of grains [8, 23]. It is followed by the dormant period with a very slow reaction (first valley). The third period is due to the acceleration of C_3S hydration that causes the second exothermal peak. The fourth period observed in this cement (third peak) is typically associated with the reaction of C_3A, and it is suggested that it corresponds to the renewed formation of Ett (AFt- phase) [8, 24]. Finally, the de-acceleration period is characterized by the slow decrease of thermal signal.

For the selected times marked in the calorimetric curve (Fig. 2a), the XRD patterns for pastes containing PC, 30MK1, and 30MK2 are illustrated in Fig. 3.

In the PC paste (Fig 3a), the unhydrated phases of PC (C_3S, C_2S, C_3A, and C_4AF) were identified coexisting with gypsum during the dormant period (3 h). Some Ett and portlandite (CH) are identified at very early age, but the intensity of their peaks is very low. The second calorimetric peak starts at 3 h having the maximum at ~12 h, and the slope of calorimetric during the accelerating period is 0.50 J g^{-1} h^{-2}. During the acceleration period, XRD patterns (3–12 h—Fig. 3a) show that the intensity of C_3S-peaks decreases with the consequent increase of the intensity of CH peaks, while those assigned to C_2S remain. The formation of C–S–H phase, a poorly crystalline compound, cannot be identified by XRD. In this period, the intensity of Ett peaks also increases, and gypsum cannot be identified at 12 h.

After the C_3S hydration peak, the calorimetric curve shows the third peak that has the maximum at ~19 h with an upward slope of 0.09 J g^{-1} h^{-2}. For the PC used with medium C_3A content (~8 %) and normal content of

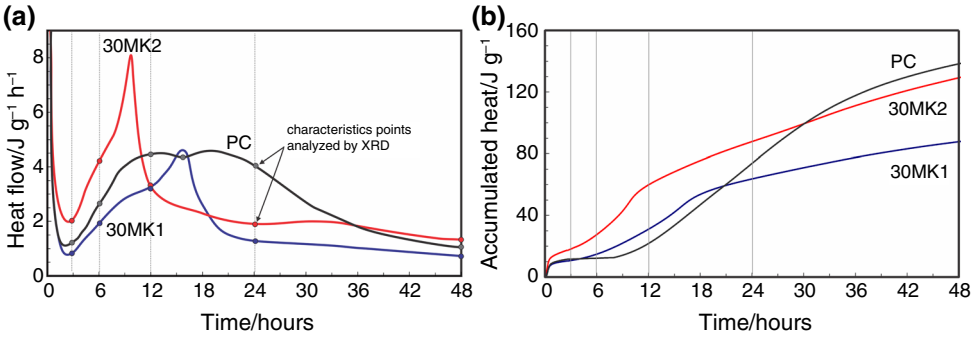

Fig. 2 Results of isothermal calorimetric test up to 48 h: **a** heat flow and, **b** accumulated heat

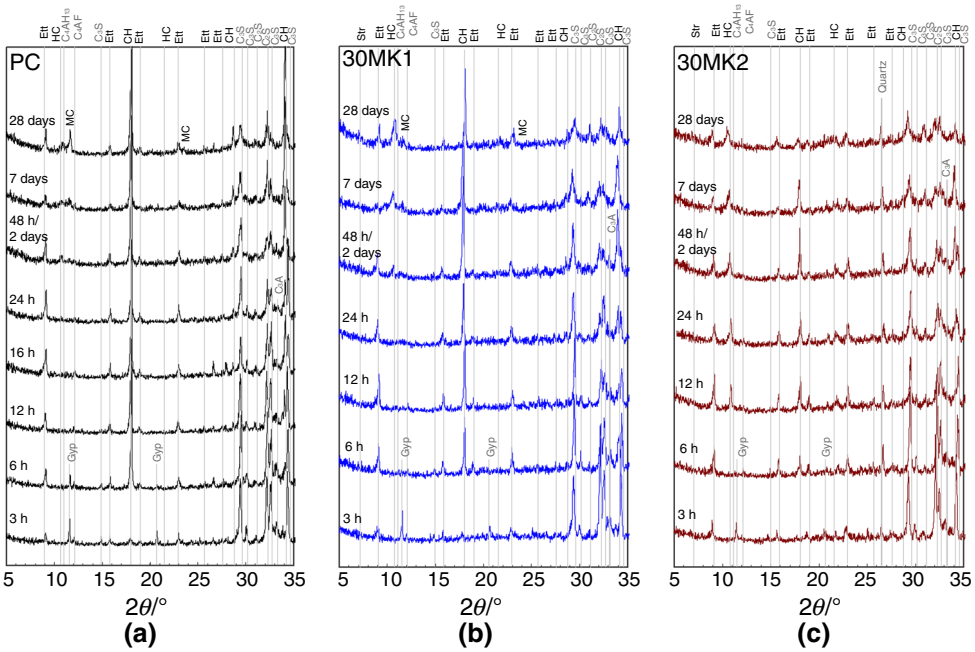

Fig. 3 XRD pattern for hydrated pastes: **a** PC; **b** 30MK1 and **c** 30MK2

gypsum (3.2 % of SO_3), this third peak is attributed to the point of exhaustion of solid gypsum that causes the acceleration of the aluminate-hydrated phase [25, 26]. After 12 h, the gypsum is absent in the XRD-pattern, and the main changes that occur from 12 to 24 h (Fig. 3a) are that the C_3A phases decrease until peaks disappear and that the main aluminate hydration product is Ett formed from sulfate previously absorbed in the C–S–H phase, according to Gallucci et al. [26].

During the de-acceleration period, no characteristic points are detected. XRD patterns during this period (24–48 h in Fig. 3a) show the formation of AFm-phase assigned as calcium hemicarboaluminate (HC: $C_3A.CH_{0.5}C\underline{C}_{0,5}.H_{12}$) with more intense peaks at 48 h.

The calorimetric curves of both blended cements show the five periods of hydration during the first day (Fig. 2a). The dissolution and dormant periods have the same duration than those in PC paste, but the acceleration period can be faster and shorter depending on the type of MK used. For 30MK2, the exothermic signal during the dormant period was higher than that of PC paste, while it was lower for the 30MK1. The XRD-pattern at 3 h shows low intensity of the peaks assigned to the gypsum, and greater intensity of those assigned to Ett in the 30MK2 paste (Fig. 3b, c).

For 30MK1-blended cement, the acceleration slope is 0.35 J g^{-1} h^{-2} showing that the hydration rate is lower than that of PC. The maximum of the second calorimetric peak occurs in advance (1 h) compared with the PC paste, and its intensity was 30 % lower than the one corresponding PC due to the dilution effect. The third calorimetric peak (Fig. 2a) is sharper and narrower, and it occurs earlier ($\sim$3 h before than PC). It has the same intensity as in PC paste, and the slope of heat release is four times greater (0.37 J g^{-1} h^{-2}). Figure 3b shows the XRD corresponding to 3, 6, 12, 24, and 48 h of hydration. As in the case of PC, Ett and CH are detected at the early hours. During the acceleration period, the intensity of C_3S peaks decreases, and that of CH increases indicating the progress of cement hydration. Before and after the aluminate peak,

the alumina-hydrated phase detected by XRD is Ett, and only the C_3A-peak disappears. This observation confirms that the third peak corresponds to the second formation of Ett [25]. At 48 h, the hemicarboaluminate (HC) was detected as well as in PC paste, indicating that when the sulfate is exhausted; some parts of alumina remain unreacted; and the first phase of transformation from AFt to AFm occurs.

For 30MK2-blended cement, the second calorimetric peak occurs earlier than in PC paste, and the acceleration slope (0.82 J g^{-1} h^{-2}) is much higher than that of PC (Fig. 2a). The third calorimetric peak occurs early at 10 h (~9 h before PC), and its intensity is stronger (Fig. 2a) with an exothermic rate of 1.62 J g^{-1} h^{-2}. This value is eighteen and four times higher than the one corresponding to PC and MK1, respectively. After this peak, the deacceleration is too fast.

Fig. 3c shows the XRD patterns corresponding to 3, 6, 12, 24, and 48 h of hydration of 30MK2 cement. During the acceleration period (between 3 and 6 h), the hydrated compounds detected were Ett and CH. After the third calorimetric peak (12 h), the intensity of Ett peaks in XRD is higher than that determined in the other pastes, but it is accompanied by a well-defined peak of the AFm phase (assigned as calcium hemicarbonate). The intensity of the CH-peaks is lower than that corresponding to PC or 30MK1, showing a little CH-consumption to form C–S–H and C–A–H phases by the pozzolanic reaction. Therefore, Ett and HC remain as crystalline phases. The HC phase is formed in the pozzolanic reaction between the reactive alumina from the pozzolan, and the CH and $C\underline{C}$ from the limestone filler [27], a minor component in the PC used.

Up to 48 h, Fig. 2b shows that accumulated heat released by 30MK1 was always lower than that of PC, indicating that the dilution effect is predominant for this addition, and that a lower compressive strength is expected. For 30MK2-blended cement, the accumulated heat was higher than that of PC up to 22 h indicating the stimulation effect on the PC hydration caused by this addition. After 2 days, the accumulated heat values were 143.4, 87.7, and 129.2 J g^{-1} for PC, 30MK1, and 30MK2, respectively. These values correspond to 0.61 and 0.90 of the accumulated heat of PC for 30MK1 and 30MK2, respectively.

The calorimetric analysis clearly differentiates the reactivity of both kaolinitic-calcined clays. Similar results were reported by Lagier and Kurtis [8] using a Portland cement with medium C_3A content (Cement 2) with 8 % of metakaolin with similar mineralogical composition, but a different specific surface area. For samples analyzed in this paper, the structural order of kaolinite in K1-clay determines a MK1 with less specific surface area, high d_{90}, and less access points for the pore solution. Therefore, it has a low early reactivity up to 12 h, which causes the reduction in the accumulated heat due to the dilution effect. The increase in the slope corresponding to the third peak of the calorimetric curve could be attributed to the early SO_4^{2-} depletion in the pore solution by adsorption that causes the high specific surface area of mineral addition. MK2 presents a high specific surface area and more access points for the pore solution due to the original structural disorder of kaolinite in K2-clay, causing an acceleration of the hydration at early age. The large specific surface area of MK2 also develops a more pronounced and intense third peak, which may be attributed to the formation of aluminate phases, similar to that occurred in Portland cement with medium or high C_3A content blended with mineral addition having a large specific surface area, such as silica fume [28].

Hydration at later age

Figure 4 shows the DTA analyses for PC, 30MK1, and 30MK2 pastes obtained at 2, 7, and 28 days, respectively. Kuliffayová et al. [29] reported that the DTA curves indicate four endothermic peaks at 120–260, 300–440, 450–530, and 530–900 °C. The first two endothermic peaks located at about 120–440 °C characterize the dehydration of the C–S–H, C–A–H, and C–S–A–H compounds. The endothermic peak observed at about 450–530 °C is characteristic of the CH dehydroxilation. The last endothermic peaks that appeared at about 530–900 °C represent the decomposition of calcium carbonates. Ettringite suffers loss water at a very low temperature (~40 °C), and its complete decomposition into gypsum, hemihydrate (C–A–H) together with an amorphous material that occurs at 120 °C [30]. According to Morsy [31], the first peak located within 110–120 °C is mainly due to the dehydration of C–S–H, and the peaks observed around 160, 210, and 310 °C represent the decompositions of C–A–H and C–A–S–H. However, these peaks cannot be divided to quantify the phases. Depending on literature, the CH dehydroxylation occurs at around 470 °C [31], at about 440–530 °C [29], or at 450–600 °C [25]. Finally, decomposition of carbonates shows peaks in the temperature range of 625–875 °C in the hydrated samples. However, the decarbonation at 2 and 7 days occurred at a lower temperature. This fact can be related to the presence of different types of carbonates, different contents, or different crystallinity degrees. [32]. In this study, the temperature range for TG calculations was adopted as 110–440 °C for dehydration of C–S–H, C–A–H, and C–A–S–H phases including HC and Ett in the C–A–H group, and 440–560 °C for CH dehydroxylation. Table 4 reports the percentages of mass loss corresponding to these temperature ranges. Complementarily, the crystalline phases (especially, the CH, C–A–H and C–A–S–H phases) were identified by XRD analysis at 7 and 28 days (Fig. 3).

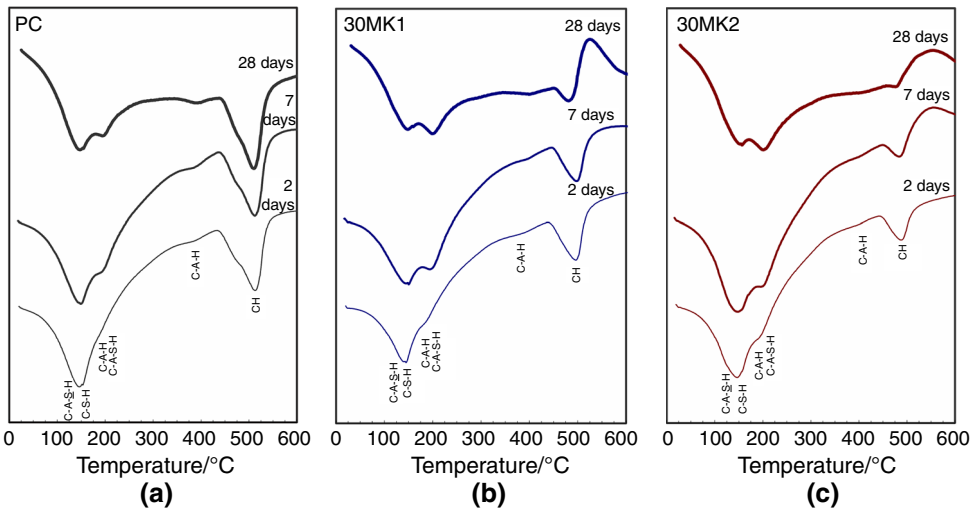

Fig. 4 DTA curves for hydrated pastes: **a** PC; **b** 30MK1, and **c** 30MK2

Table 4 Percentages of mass loss determined by DTA/TG

Cement	Age	Mass loss/ %	
		Dehydration C–S–H, C–A–H, C–A–S–H 110–440 °C	Dehydroxylation CH 440–560 °C
PC	2	9.7	3.3
	7	11.7	3.9
	28	12.2	3.9
30MK1	2	7.8	2.1
	7	10.9	2.0
	28	10.1	0.7
30MK2	2	10.4	1.4
	7	14.1	1.2
	28	14.2	0.5

From the curve of PC-paste (Fig. 4a), the areas and intensities of the characteristic peaks typical of C–S–H/C–A–H and CH increase with the increasing hydration age. At 2 days, the first endothermic peak cannot distinguish between the peak corresponding to C–S–H and the peak of aluminic phase, which appears as a shoulder at 7 days. Both peaks can be clearly differentiated at 28 days. These results agree with the XRD analyses (Fig. 3a) where it is possible to identify the AFm phases corresponding to HC and MC (monocarboaluminate) at 7 and 28 days. The endothermic peak of C–S–H (145 °C) is more intense than the one corresponding to alumina phases (195 °C) at a later age (28 days). The endothermic peak (380–410 °C) corresponding to the decomposition of hydrogarnet (C_3AH_6) [29] was detected with the increasing intensity from 2 to 28 days. However, hydrogarnets are not identified in the XRD patterns.

From the curve of 30MK1 and 30MK2 pastes (Fig. 4b, c), the different reactivities of these additions can be evaluated by the intensity and the area of the first and CH peaks. At 2 days, the peaks of CH and C–S–H/C–A–H/C–A–S–H of the 30MK1 paste have a smaller area and intensity than the ones corresponding to the PC paste. This is due to the dilution effect and the slow reaction of MK1. For MK2, the area of CH peak is too small, but the first peak present in the curve has a similar area to the corresponding to PC. In this peak, the maximum is at 150 °C, and a shoulder assigned to aluminic phase is detected in accordance with a well-developed peak of HC in the XRD pattern (Fig. 3c). These results also agree with the accumulated heat reported at 48 h: 30MK1 paste has lower accumulated heat than the one corresponding to PC, and 30MK2 is close to PC (Fig. 2b).

At 7 and 28 days, the decrease in the peak area of CH, as shown in XRD patterns (Fig. 3b, c), is the main feature in the curve of blended cements. This reduction is more pronounced for the 30MK2-blended cement indicating a large progress of pozzolanic reaction. The reaction products formed during the pozzolanic reaction are C–S–H, C–A–H, and C–A–S–H [Eqs. (1) and (2)] producing increases in the area and the intensity of the first peaks. At 7 days, the peak of C–A–H/C–A–S–H phases is well defined and more pronounced than the one corresponding to C–S–H at 28 days. C–A–H/C–A–S–H phases are identified as HC and strätlingite (C_2ASH_8) by XRD, and the intensities of the peaks are more pronounced for 30MK1 paste. For 30MK2, the area of the first peak is larger than the ones corresponding to PC and 30MK1 pastes indicating higher amounts of these phases, but they have lower crystallinity according to the XRD pattern at 28 days (Fig. 3c).

For the PC paste, the mass loss is attributed to C–S–H/C–A–H, and CH increases with the hydration progress. The C–S–H and CH contents increase due to the progression of C_3S and C_2S hydration, and the C–A–H phases (derived from C_3A and C_4AF hydrations) identified by XRD

Table 5 Compressive strength, strength activity index (SAI) and calorimetric activity index (CAI)

Cement	**Age**/days	**Compressive strength**/MPa	**SAI**	**CAI**
PC	2	25		
	7	30.6		
	28	38.4		
30MK1	2	14.9	0.60	0.61
	7	26.1	0.85	
	28	33.9	0.88	
30MK2	2	21.2	0.85	0.90
	7	34.9	1.14	
	28	48.8	1.27	

(HC: $C_3A.CH_{0.5}C\underline{C}_{0,5}.H_{12}$, MC: $C_3A.C\underline{C}.H_{12}$, C_4AH_{13}= $C_3A.CH.H_{12}$) lose approximately the same amount of water during their decomposition and in the same temperature range. [24].

For both blended cements, CH decreases (Table 4) from 2 to 28 days. For 30MK1, the amount of CH is lower than the 70 % of CH in PC, evidencing a pozzolanic reaction as reported previously [7], but the amount of cementing compounds is lower than in PC (Table 5). This behavior is more evident for 30MK2, which causes a great reduction on CH-content and a large amount of hydrated phases compared with PC. At 28 days, the amount of mass loss corresponding to dehydration of C–S–H/C–A–H/C–A–S–H phases decreases slightly for 30MK1 paste.

For pastes containing kaolinitic-calcined clays, the C–S–H phase is a product from the calcium silicate hydration of Portland cement and the pozzolanic reaction between the metakaolinite and the CH released from silicates' reaction [6]. The stability of C–A–H phases (Ett, C_4AH_{13} and HC) formed at early ages during cement hydration or pozzolanic reaction depends on the availability of other ions (CO_3^{2-}, SO_4^{2-}, etc.) and the amount of CH in the system [6]. C_4AH_{13} is the crystalline phase (C–A–H) formed by metakaolinite reaction when the CH is largely available [6]. When cement contains a small proportion of limestone filler, C_4AH_{13} is stabilized as HC [25, 27]. For highly reactive kaolinitic-calcined clays, the amount of CH decreases to a very low amount, and the crystalline phase found is Str obtained from the substitution of calcium by silicon at later age [6]. In Fig. 3b, c, HC and Str were identified by XRD in 30MK1 and 30MK2 pastes at 28 days. The more stable C–A–S–H phase is the $C_3AS_{3-x}H_{2x}$, with x: 0 to 3 (hydrogarnet), formed at very later ages or in paste hydrated at high temperatures [27, 33, 34]. Then, this phase detected by DTA is attributed to the thermal decomposition of the AFt and AFm phases [35].

Then, the mass loss that occurs due to dehydration of C–S–H/C–A–H/C–A–S–H phases is highly influenced by the amount of chemical-combined water in the structure and varies according to the aluminic phases present for each paste and age. On the other hand, the mass loss due to dehydroxylation of CH is directly proportional to the mass of this phase in the paste.

Compressive strength

Table 5 shows the values of the compressive strength and the pozzolanic activity index (SAI) at 2, 7, and 28 days for mortars. In this table, the pozzolanic activity index determined from calorimetric (CAI) at 2 days is also reported. For 30MK1-blended cement, the compressive strength was always lower than the one corresponding to PC, corroborating the slow pozzolanic reaction due to the high structural order that causes a low specific surface area and low number of access points. Complementarily, the coarser particle size distribution obtained for this type of calcined clays could contribute to the slow reaction. At 2 days, the SAI is lower than 0.70 due to the dilution effect, as occurred for the accumulative heat value determined by calorimetric test (Table 5). Later, the SAI value increases, but it is lower than 1.0. For 30MK2, the SAI value is 0.85 at 2 days, and the relative accumulated heat is high due to the high proportion of aluminate phases formed, releasing a large heat of hydration and the large specific surface area that promotes this reaction (Table 3). Therefore, the compressive strength of 30MK2 mortar exceeds the compressive strength of PC, and the SAI is higher than 1. For cement paste, the mechanical behavior is related to the increase of the compounds that dehydrated in the first peak of curve, such as C–S–H and C–A–H (HC, MC, Ett, and C_4AH_{13} phases). Therefore, the amount of hydrated phases obtained as a result of the pozzolanic reaction, measured as water loss between 110 and 440 °C, presents a good correlation with the SAI. However, results have to be compared with caution since the mass loss of C–A–H/C–A–S–H phase depends on the combined water in the compounds. For example, in 30MK1, the change of C–A–H/C–A–S–H phase from HC to strätlingite causes a low mass loss at 28 days, while the SAI increases between 7 and 28 days. For MK2, it does not occur so, due to the different assemblages of hydrates.

Conclusions

On the basis of the thermal analysis, the following conclusions were drawn:

- The content and the structural order/disorder degree of kaolinite in clays can be determined by DTA/TG

analysis determining the mass loss from 500 to 750 °C and the slope ratio index of this peak.

- The DTA technique is suitable to select the calcination temperature for complete dehydroxylation of kaolinite, and the best temperature depends on the kaolinite structure.
- Calorimetric analysis of blended cements can clearly differentiate the reactivities of the calcined clays with high content of metakaolinite. More reactive calcined clay (MK2) develops the second and third peaks, earlier than those of PC with greater intensity and high acceleration. This sample from kaolinite with high structural disorder has a large specific surface area, high grindability, and small mean particles size (d_{50}) for the same sieve-retained objective in the grinding.
- The calorimetric activity index (CAI) can be used to calculate the early pozzolanic activity with results similar to those obtained by the compressive strength index (SAI).
- The DTA/TG analysis, complemented with XRD, allows determining the type and the amount of hydrated phases at different ages to evaluate the pozzolanic reaction of calcined clay. Results show that the amount of CH decreases, and the amounts of C–S–H/C–A–H phases (measured as the mass loss between 110 and 440 °C) increase with the progress of pozzolanic reaction. These values are correlated with the increase of the pozzolanic activity index measured by the compressive strength.

References

1. Habert G, Billard C, Rossi P, Chen C, Roussel N. Cement production technology improvement compared to factor 4 objectives. Cem Concr Res. 2010;40:820–6.
2. Yang KH, Hwang HZ, Kim SY, Song JK. Development of a cementless mortar using hwangtoh binder. Build Environ. 2007;42:3717–25.
3. Badogiannis E, Kakali G, Tsivilis S. Metakaolin as supplementary cementitious material. Optimization of kaolin to metakaolin conversion. J Therm Anal Calorim. 2005;81:457–62.
4. Cherem da Cunha AL, Gonçalves JP, Büchler PM, Dweck J. Effect of metakaolin pozzolanic activity in the early stages of cement type II paste and mortar hydration. J Therm Anal Calorim. 2008;92:115–9.
5. Siddique R, Klaus J. Influence of metakaolin on the properties of mortar and concrete: a review. Appl Clay Sci. 2009;43:392–400.
6. Murat M. Hydration reaction and hardening of calcined clays and related minerals. I. Preliminary investigation on metakaolinite. Cem Concr Res. 1983;13:259–66.
7. Tironi A, Trezza MA, Scian AN, Irassar EF. Kaolinitic calcined clays: factors affecting its performance as pozzolans. Constr Build Mater. 2012;28:276–81.
8. Lagier F, Kurtis KE. Influence of Portland cement composition on early age reactions with metakaolin. Cem Concr Res. 2007;37:1411–7.
9. Andreis RR. Diagénesis y arcillas intersiciales en las unidades neopaleozoicas del grupo Paganzo—La Rioja. Rev As Geo Arg. 2006;61:364–9.
10. Volkheimer W. Observaciones geológicas en el área de Ingeniero Jacobacci y adyacencias (Provincia de Río Negro). Rev As Geo Arg. 1973;28:13–36.
11. EN 197-1:2011. Cementos comunes: composición, especificaciones y criterios de conformidad.
12. Shvarzman A, Kovler K, Grader GS, Shter GE. The effect of dehydroxylation/amorphization degree on pozzolanic activity of kaolinite. Cem Concr Res. 2003;33:405–16.
13. Bich Ch, Ambroise J, Péra J. Influence of degree of dehydroxylation on the pozzolanic activity of metakaolin. Appl Clay Sci. 2009;44:194–200.
14. Kingery WD, Bowen HK, Uhlmann DR. Introduction to ceramics. 2nd ed. New York: Wiley; 1976.
15. Wilson MJ. A Handbook of determinative methods in clay mineralogy. New York: Chapman and Hall Publications; 1987.
16. Aparicio P, Galan E. Mineralogical interference on kaolinite crystallinity index measurements. Clays Clay Miner. 1999;47:12–27.
17. He H, Yuan P, Guo J, Zhu J, Hu C. The influence of random defect density on the thermal stability of kaolinites. J Am Ceram Soc. 2005;88:1017–9.
18. ASTM C204-11. Standard test methods for fineness of hydraulic cement by air-permeability Apparatus.
19. Kogel JE, Trivedi NC, Barker JM, Stanley TK. Industrial minerals & rocks. 7TH ed. Englewood: Society for Mining, Metallurgy, and Exploration; 2006.
20. Tironi A, Trezza MA, Irassar EF, Scian AN. Thermal treatment of kaolin: effect on the pozzolanic activity. Proc Mater Sci. 2012;2012(1):343–50.
21. Tironi A, Trezza MA, Irassar EF, Scian AN. Tratamiento térmico de arcillas caoliníticas para su utilización como puzolanas. Libro de las XI Jornadas Argentinas de Tratamiento de Minerales; 2012:115–120.
22. Balek V, Murat M. The emanation thermal analysis of kaolinite clay minerals. Thermochim Acta. 1996;282(283):385–97.
23. Quennoz A, Scrivener KL. Hydration of C_3A–gypsum systems. Cem Concr Res. 2012;42:1032–41.
24. Taylor HFW. La química de los cementos, Enciclopedia de la industria química. Ed. URMO, Spain; 1967.
25. Antoni M, Roseen J, Martirena F, Scrivener K. Cement substitution by a combination of metakaolin and limestone. Cem Concr Res. 2012;42:1579–89.
26. Gallucci E, Mathur P, Scrivener K. Microstructural development of early age hydration shells around cement grains. Cem Concr Res. 2010;40:4–13.
27. Matschei T, Lothenbach B, Glasser FP. The AFm phase in Portland cement. Cem Concr Res. 2007;37:118–30.
28. Rahhal V, Talero R. Calorimetry of Portland cement with silica fume, diatomite and quartz additions. Constr Build Mater. 2009;23:3367–74.
29. Kuliffayová M, Krajči Ĺ, Janotka I, Šmatko V. Thermal behaviour and characterization of cement composites with burnt kaolin sand. J Therm Anal Calorim. 2012;108:425–32.
30. Zhou Q, Glasser FP. Thermal stability and decomposition mechanisms of ettringite at <120 degrees C. Cem Concr Res. 2001;31:1333–9.
31. Morsy MS. Effect of temperature on hydration kinetics and stability of hydration phases of metakaolin-lime sludge-silica fume system. Ceram Silik. 2005;49:225–9.
32. Hidalgo A, García JL, Cruz Alonso M, Fernández L, Andrade C. Microstructure development in mixes of calcium aluminate cement with silica fume or fly ash. J Therm Anal Calorim. 2009;96:335–45.

33. Frías M, Cabrera J. Influence of MK on the reaction kinetics in MK/lime and MK-blended cement systems at 20 °C. Cem Concr Res. 2001;31:519–27.
34. Frías Rojas M. Study of hydrated phases present in a MK-lime system cured at 60 °C and 60 months of reaction. Cem Concr Res. 2006;36:827–31.
35. Meller N, Kyritsis K, Hall Ch. The hydrothermal decomposition of calcium monosulfoaluminate 14-hydrate to katoite hydrogarnet and beta-anhydrite: an in-situ synchrotron X-ray diffraction study. J Solid State Chem. 2009;182:2743–7.